($e^{2i\alpha} = z^2r^{-2}$) and σ_{xx}, σ_{yy}, τ_{xy} (see Fig. 2) according to the same formulas for $\alpha = 0$. The computations were performed for $\varkappa_1 = \varkappa_2 = 2$; $\gamma = 3^{-1}$; 3; $z_2 = 1.001R_2$. The solid lines in Figs. 1 and 2 are $\gamma = 1/3$, the dashes are $\gamma = 3$, and the superscripts $j = 0, 1, 2$ correspond to the domains D_2^+, D_2^-, D_1^-.

LITERATURE CITED

1. N. I. Mushkhelishvili, Certain Fundamental Problems of Mathematical Elasticity Theory [in Russian], Nauka, Moscow (1966).
2. D. Eshelby, Continual Theory of Dislocations [Russian translation], IL, Moscow (1963).
3. D. V. Vainberg and A. G. Ugodchikov, "Bending stresses in a thin slab under connections with clearance," Prikl. Mekh. (Akad. Nauk UkrSSR), 4, No. 4 (1958).
4. A. G. Ugodchikov, "Stress determination during pressing of circular washers in a plate bounded by a curve of particular form," Dokl. Akad. Nauk SSSR, 77, No. 2 (1951).
5. P. I. Perlin and L. F. Tolchenova, "Containers for flat ingots," Trudy VNIImetmash., No. 1 (1960).
6. V. S. Kolesov and L. G. Smirnov, "Temperature stresses in a half-plane with an arbitrary inclusion," Mat. Metody Fiz-Mekh. Polya., No. 2 (1982).

VIBRATIONS OF AN ELASTIC ORTHOTROPIC LAYER WITH A CAVITY

A. O. Vatul'yan and A. Ya. Katsevich

UDC 539.3

In connection with the development of vibrational seismographic prospecting and defectometry at the present time, problems of analyzing wave fields in an elastic medium with cavities, cracks, and inclusions became extremely urgent. Let us note that certain materials being tested are anisotropic (austenite class steels, composites, soils) which requires an appropriate mathematical model that takes account of the anisotropy of the mechanical properties.

1. The steady-state antiplane waves are investigated in an orthotropic elastic layer of thickness h with a cylindrical cavity whose directrix is a smooth closed curve ℓ_0. We consider that the vibrations in the layer are excited by a tangential load $p(x_1)$ applied to the boundary $x_3 = h$ of the layer. The axes of elastic symmetry agree with the coordinate axes, the component $u_2 = u(x_1, x_3)\exp(-i\omega t)$ of the displacement vector components is different from zero while similarly $\sigma_{12} = c_{66}u_{,1}$, $\sigma_{23} = c_{44}u_{,3}$ from the stress tensor components. After extraction of the time factor the boundary value problem has the form

$$\begin{gathered} c_{66}u_{,11} + c_{44}u_{,33} + \rho\omega^2 u = 0, \\ x_3 = h,\ c_{44}u_{,3} = p(x_1),\ x_3 = 0,\ u = 0, \\ (x_1,\ x_3) \in l_0,\ c_{66}u_{,1}n_1 + c_{44}u_{,3}n_3 = 0 \end{gathered} \tag{1.1}$$

(n_1, n_3 are components of the unit vector normal to the curve ℓ_0, external relative to the domain occupied by the elastic medium). Formulation of the problem is closed by the radiation condition for whose formulation the limit absorption principle is used.

We introduce an auxiliary boundary value problem for the function $U(x_1, x_3, \xi_1, \xi_3)$ into the consideration

$$\begin{gathered} c_{66}U_{,11} + c_{44}U_{,33} + \rho\omega^2 U = -\delta(x_1 - \xi_1,\ x_3 - \xi_3), \\ x_3 = h,\ U_{,3} = 0,\ x_3 = 0,\ U = 0. \end{gathered} \tag{1.2}$$

The solution of the problem (1.2) is constructed by using a Fourier integral transform within

Rostov-on-Don. Translated from Zhurnal Prikladnoi Mekhaniki i Tekhnicheskoi Fiziki, No. 1, pp. 95-97, January-February, 1991. Original article submitted December 15, 1988; revision submitted July 20, 1989.

0021-8944/91/3201-0090$12.50

the framework of the limit absorption principle

$$U(x_1, x_3, \xi_1, \xi_3) = \frac{1}{4\pi c_{44}} \int_\sigma \exp(i\alpha_1(\xi_1 - x_1))\lambda^{-1}\Big[\exp(-\lambda|\xi_3 - x_3|) - \\ - \exp(-\lambda\xi_3)\operatorname{ch}\lambda x_3 + \frac{\operatorname{sh}\lambda x_3}{\operatorname{ch}\lambda h}\langle\exp(\lambda(\xi_3 - h)) + \operatorname{sh}\lambda h\exp(-\lambda\xi_3)\rangle\Big]d\alpha_1, \tag{1.3}$$

where $\lambda = (\nu\alpha_1^2 - k^2)^{1/2}$; $\nu = c_{66}/c_{44}$; $k^2 = \rho\omega^2/c_{44}$, the contour σ is selected in conformity with the limit absorption principle and envelops the positive pole and the branch point of the integrand from below, and the negative from above [1]. Using the reciprocity theorem [2], it is easy to obtain a representation of the displacement field in the medium

$$u(\xi_1, \xi_3) = \int_{R_1} p(x_1)U(x_1, h, \xi_1, \xi_3)\,dx_1 - \int_{l_0}\Big[c_{66}n_1\frac{\partial U}{\partial x_1}(x_1, x_3, \xi_1, \xi_3) + c_{44}n_3\frac{\partial U}{\partial x_3}(x_1, x_3, \xi_1, \xi_3)\Big]u(x_1, x_3)\,dl_x. \tag{1.4}$$

If we determine $u(x_1, x_3)$ for $(x_1, x_3) \in \ell_0$, then (1.4) permits finding the displacement everywhere within the domain occupied by the elastic medium.

A boundary integral equation along the boundary of the domain ℓ_0 can be formulated on the basis of (1.4) since the boundary conditions for $x_3 = 0$, h are satisfied automatically because of the special selection of the fundamental solution $U(x_1, x_3, \xi_1, \xi_3)$. Let us pass to the limit $(\xi_1, \xi_3) \to (y_1, y_3) \in \ell_0$ in (1.4). Let us introduce a local coordinate system in (y_1, y_3), let us draw a circle ℓ_ε of radius $\varepsilon > 0$, and let us find the integral over in its parts within the original elastic domain. Evaluating the integrals encountered here and taking into account that the main contribution to the limit value is given by the first component in (1.3), we obtain the following boundary integral equation in the limit

$$\frac{1}{2}u(y_1, y_3) = \int_{R_1} p(x_1)U(x_1, h, y_1, y_3)\,dx_1 - \int_{l_0}\Big[c_{66}n_1\frac{\partial U}{\partial x_1}(x_1, x_3, y_1, y_3) + c_{44}n_3\frac{\partial U}{\partial x_3}(x_1, x_3, y_1, y_3)\Big]u(x_1, x_3)\,dl_x, (y_1, y_3) \in l_0, \tag{1.5}$$

where the integral over ℓ_0 is understood in the Cauchy principal value sense.

2. Numerical realization of the singular integral equation (1.5) is on the basis of the method of boundary elements (MBE). Different modifications of the numerical realization of equations of the type (1.5) are elucidated in detail in [2, 3].

Let us use the simplest MBE modification by considering that a smooth boundary is separated into N_1 elements by rectangular segments, within whose limits $u(x_1, x_3)$ is constant while the nodes are the midpoints of the appropriate segments. Let (x_{1k}^-, x_{3k}^-) and (x_{1k}^+, x_{3k}^+) denote coordinates of the beginning and ending of the k-th element in conformity with the orientation selected. Then the node coordinates are found in the form $y_{1k} = 1/2(x_{1k}^- + x_{1k}^+)$, $y_{3k} = 1/2(x_{3k}^- + x_{3k}^+)$. For $u_k = u(y_{1k}, y_{3k})$ Eq. (1.5) reduces to a linear algebraic system

$$\frac{1}{2}u_k = b_k - \sum_{m=1}^{N_1} H_{km}u_m, \quad k = 1, 2, \ldots, N_1; \tag{2.1}$$

$$b_k = \int_{R_1} p(x_1)U(x_1, h, y_{1k}, y_{3k})\,dx_1, \tag{2.2}$$

$$H_{km} = \int_{l_m}\Big[c_{66}n_{1m}\frac{\partial U}{\partial x_1}(x_1, x_3, y_{1k}, y_{3k}) + c_{44}n_{3m}\frac{\partial U}{\partial x_3}(x_1, x_3, y_{1k}, y_{3k})\Big]dl_x.$$

Let us note that formation of the system matrix is the main difficulty since the fundamental solution $U(x_1, x_3, \xi_1, \xi_3)$ has no explicit representation and multiple integrals must be evaluated for the calculation H_{km}. Consequently, (2.2) requires preliminary simplification.

Let us introduce the parametrization

$$x_1 = y_{1m} + \beta_{1m}t, \ \beta_{1m} = \frac{1}{2}(x_{1m}^+ - x_{1m}^-), \ x_3 = y_{3m} + \beta_{3m}t,$$

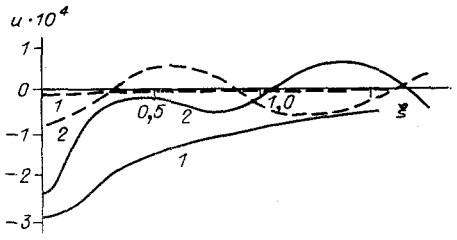

Fig. 1

$$\beta_{3m} = \frac{1}{2}\left(x_{3m}^{+} - x_{3m}^{-}\right) \tag{2.3}$$

in the element ℓ_m. Evaluating the integrals over t in (2.2) we obtain an expression for the coefficients of the linear algebraic system in the form of integrals over the contour σ

$$\begin{aligned} H_{km} = \frac{1}{4\pi}\int_{\sigma} \exp\left(i\alpha_1\left(y_{1k} - y_{1m}\right)\right)\lambda^{-1}\left\{\exp\left(-i\alpha_1\beta_{1m}t_*\right)\left(g\left(t_{km}^{-}, \alpha_1\right) - \right.\right. \\ - g\left(t_{km}^{+}, \alpha_1\right)\Big] + \exp\left(-i\alpha_1\beta_{1m} - \lambda\left|t_{km}^{+}\right|\right) g\left(t_{km}^{+}, \alpha_1\right) - \exp\left(i\alpha_1\beta_{1m} - \right. \\ - \lambda\left|t_{km}^{-}\right|\Big) g\left(t_{km}^{-}, \alpha_1\right) + 2\exp\left(\lambda\left(y_{3m} - h\right)\right)\frac{\operatorname{sh}\lambda y_{3k}\operatorname{sh}\left(\lambda\beta_{3m} - i\alpha_1\beta_{1m}\right)}{\operatorname{ch}\lambda h} g\left(1, \alpha_1\right) + \\ \left. + 2\exp\left(-\lambda y_{3m}\right)\frac{\operatorname{ch}\lambda\left(h - y_{3k}\right)\operatorname{sh}\left(\lambda\beta_{3m} + i\alpha_1\beta_{1m}\right)}{\operatorname{ch}\lambda h} g\left(1, \alpha_1\right)\right\} d\alpha_1, \\ g\left(t, \alpha_1\right) = \frac{\lambda\operatorname{sgn} t\beta_{1m} + i\alpha_1\nu\beta_{3m}}{\lambda\operatorname{sgn} t\beta_{3m} - i\alpha_1\beta_{1m}},\ t_* = \frac{y_{3k} - y_{3m}}{\beta_{3m}},\ t_{km}^{\pm} = y_{3k} - y_{3m} \mp \beta_{3m}. \end{aligned} \tag{2.4}$$

The integrals over the contour σ in the complex plane in (2.3) are evaluated according to Gauss quadrature formulas. On the basis of computations using (1.5), the wave field is constructed on the layer surface

$$\begin{aligned} u\left(\xi_1, h\right) = -TU\left(0, h, \xi_1, h\right) - \sum_{m=1}^{N_1} F_m\left(\xi_1\right) u_m \\ \left(F_m\left(\xi_1\right) = \int_{l_m}\left[c_{66}n_{1m}\frac{\partial U}{\partial x_1}\left(x_1, x_3, \xi_1, h\right) + c_{44}n_{3m}\frac{\partial U}{\partial x_3}\left(x_1, x_3, \xi_1, h\right)\right] dl_x\right) \end{aligned} \tag{2.5}$$

under the action of a concentrated load $p(x_1) = -T\delta(x_1)$ at the origin.

It is assumed in the computations that the cavity ℓ_0 is an ellipse with center at the middle of the layer (0, h/2), its semiaxes a_1 and a_3 are parallel to the coordinate axes, and the number of boundary elements is 8 and 16 while the elastic constants (in N/m^2) are $c_{44} = 7.93\cdot10^{10}$, $c_{66} = 5.05\cdot10^{10}$, $T = 10^7$. Displacement of the layer surface is computed according to (2.5) in the near zone for different values of the dimensionless parameter $\varkappa = \omega h(\rho/c_{44})^{1/2}$ corresponding to the number of modes being propagated in the layer. Let us note that the cutoff frequencies for a continuous waveguide [1] are $\varkappa_n = \pi\ (n - 1/2)$, $n = 1, 2, \ldots$.

The continuous line in Fig. 1 depicts $\operatorname{Re} u(\xi_1, h)$, and the dashes $\operatorname{Im} u(\xi_1, h)$ for the following parameter values: $a_1/h = 0.1$, $a_3/h = 0.2$, where the number 1 corresponds to $\varkappa^2 = 2$, and 2 to $\varkappa^2 = 20$. The waveguide is locked for the first value of $\varkappa$, shifts decrease exponentially with distance from the vibrations source, and the wave field is localized in the neighborhood of the cavity. The second value of $\varkappa$ corresponds to one mode being propagated. Let us note that the relative error in computing the displacement in both cases does not exceed 8% in going from $N_1 = 8$ to $N_1 = 16$.

On the basis of the relationships (1.5) and (2.5) the inverse problem of determining cavity parameters according to the wave field on a layer surface can be formulated.

LITERATURE CITED

1. I. I. Vorovich and V. A. Babeshko, Dynamic Mixed Problems of Elasticity Theory for Nonclassical Domains [in Russian], Nauka, Moscow (1979).

2. P. Banerjee and R. Butterfield, Boundary Element Methods in Engineering Science, McGraw-Hill, New York (1982).
3. D. Colton and R. Kress, Integral Equations Methods in Scattering Theory [Russian translation], Mir, Moscow (1987).

PLASTIC MACRODEFORMATION WITH TWISTING UNDER PRESSURE FOR ALUMINUM WITH LOCALLY INTRODUCED GRAPHITE POWDER

V. V. Neverov

UDC 529.37

A description of plastic deformation of crystalline solids is given within the scope of dislocation theory and solid mechanics. Physical theories which describe microdeformation do not give a straightforward representation of a body as a whole since they cannot describe macrodeformation. The problem of combining these theories can only be solved taking account of the hierarchy of the scale levels for deformation [1]. The combination is supported by a weak experimental study of macroscopic deformation levels. As a rule deviation of macroscopic movements from laminar paths predicted by solid mechanics is small with normal plastic deformation schemes. Therefore in order to observe them methods are required which make it possible not only to carry out recording in large fields, but also quite fine fields [2]. However, another way is possible, i.e., by increasing the level of plastic deformation and property inhomogeneity for specimens. Development of macromovements is strengthened, which simplifies observing them. Macromovements and convective mass transfer in short cylindrical specimens of aluminum containing locally introduced graphite powder with plastic deformation in twisting under pressure are described and discussed. The study is also of interest in connection with the problem of preparing alloys by means of plastic deformation [3].

Study Procedure. Tests were performed in a "shear under pressure" device [3] with a restraining ring which made it possible to increase specimen thickness h to 3 mm with a piston diameter of $2R = 8$ mm. After prior compression holes were drilled in the specimen parallel to the axis of rotation and they were filled with graphite powder with a particle size <0.5 mm. In other tests the powder was distributed in a thin layer within a specimen over a surface perpendicular to the axis of rotation. Then the cell was closed by the piston, a compressive pressure of 1 GPa was applied, and the piston was rotated to the prescribed number of rotations n. The rate of piston rotation $\dot{\varphi} = 0.14$ sec^{-1} which excluded specimen heating [4]. In order to provide parallelness for the specimen ends all of the device component surfaces transmitting a compressive force were ground for parallelness from both sides. Both cylinders, i.e., the cylinder with the piston and the cylinder at the end of which the specimen was placed in the restraining ring, were located in a guidance housing. The diameter of the housing exceeded that of the cylinders by not more than $a = 4 \cdot 10^{-2}$ mm. During tests the housing could rotate freely and therefore the slope of the cylinder axes did not exceed $\alpha = 2a/H \approx 2 \cdot 10^{-3}$, where H is cylinder height. Microsections were prepared from deformed specimens, the position of the graphite in them was observed from which material movement was assessed, and the microhardness was measured. Macromovements were compared with those calculated for a viscoplastic material model.

Results of Observations. In the first piston rotations with $n < 10$ a column of graphite was transformed into a screw-shaped band and from its pitch the distribution of displacements through the specimen thickness was found (Fig. 1a, $n = 8$, graphite in one hole $\varnothing = 1$ mm at a distance from the axis $r_0 = 3$ mm; Fig. 1b, the same as for 1a but before introducing the graphite the aluminum was deformed with $n = 20$; all photographs magnified by eight).

Novokuznetsk. Translated from Zhurnal Prikladnoi Mekhaniki i Tekhnicheskoi Fiziki, No. 1, pp. 98-103, January-February, 1991. Original article submitted April 18, 1989; revision submitted July 20, 1989.

0021-8944/91/3201-0093$12.50